

Optimization of photo-Fenton to work at neutral pH using NTA–Fe²⁺

Jaime Gil Cortes, Renato F. Dantas*

School of Technology, University of Campinas, Paschoal Marmo 1888, Limeira, Brazil, Tel. +55 19 21133305; Fax: +55 19 21133305; emails: renatofalcaod@ft.unicamp.br (R.F. Dantas), jaime0_31@hotmail.com (J.G. Cortes)

Received 23 April 2019; Accepted 23 July 2019

ABSTRACT

The potential of photo-Fenton treatment to remove organic pollutants was already demonstrated in the last decades. However, the strategies to perform it at neutral pH are frequently associated with the reduction in efficiency when compared to the system performed at pH around 3. The objective of this work was to study the color removal optimization at acidic and neutral pH using NTA–Fe²⁺ complex with posterior application for the disinfection of a secondary effluent. The Doehlert matrix and the rotatable central compound designs were used for the system optimization and H₂O₂, Fe²⁺ and dye concentrations were used as variables. The importance of each variable for the system at neutral and acidic pH was analyzed by means of Pareto charts and their relations were analyzed by the response surface methodology. The optimized conditions using NTA–Fe were able to achieve a reduction of more than 4 logs in total coliforms and 6 logs for *E. coli* at the end of 60 min of treatment.

Keywords: Optimization; Chelation; Advanced oxidation; Effluent treatment; NTA

1. Introduction

Advanced oxidation processes (AOPs) are proposed as alternative treatments for the removal of organic contaminants and disinfection of wastewater. These processes have the advantage of generating highly reactive radicals, most of the time by the interaction of UV radiation with chemical agents. The formed radicals are able to oxidize organic and inorganic compounds, mainly those resistant to conventional treatments [1–4]. Among AOPs, the Fenton process appears as an interesting and simple alternative. It is based on electron transfer between the hydrogen peroxide (H₂O₂) and a metal catalyst (Fe²⁺) to produce hydroxyl radicals (HO•). This reaction is propagated by the regeneration of Fe²⁺ due to the reduction of Fe³⁺, thus generating highly oxidizing radicals [5–7]. The use of Fenton reaction combined with UV or solar light to improve the process is known as photo-Fenton. Many aspects of it have already been studied such as catalyst concentration, effects of salts presence and H₂O₂ concentration.

In addition, the removal of different types of pollutants, that is, pesticides and pharmaceuticals has been evaluated and found to present good results [8–12].

Since Fenton and photo-Fenton process uses Fe²⁺ as catalyst, its precipitation in the medium is prevented by performing the treatment in acidic medium, generally pH around 3 [13–15]. Nowadays, photo-Fenton became an efficient method to treat effluents containing different types of contaminants [16,17]. Despite the remarkable benefits of this process, its use is still limited due to the high operating costs related to the short pH range to which it has to work. Thus, the acidification of the medium and subsequent neutralization is an important drawback for its application in real wastewater [18,19]. In this context, the scientific community has been looking for strategies to perform it at circum-neutral pH in order to make it feasible to treat wastewater.

In the last decade, organic chelates have been used in order to increase the solubility of the metals and avoid their precipitation in waters near neutral pH, making possible

* Corresponding author.

the treatment of effluents with circumneutral pH [20–22]. In a recent work, nitrilotriacetic acid (NTA) was used as chelating agent to avoid iron precipitation, obtaining good results using molar proportions of 1:1.5 of Fe:NTA [23].

To perform photo-Fenton using chelating agents with maximum efficiency, the variables of the system need a proper optimization. Fe^{2+} , H_2O_2 and chelant concentration need to be adjusted to the best value, since unnecessary amount of chelant can add to the system additional organic matter, increase toxicity and cause remobilization of metals after the effluent disposal. Multivariate experimental design allows the optimization of more than one variable at the same time, thus reducing the number of experiments and saving time and resources. The rotatable central compound designs (RCCD) provide suitable results requiring a small number of experiments, while the Doehlert matrix (DM) offers the possibility of reusing the same experiments even though the limits have not been well chosen at first [24–26].

The aim of this study was to optimize the photo-Fenton process in terms of HO^\bullet radical production at acidic pH, in this case represented by methylene blue (MB) removal. Afterwards, the system was optimized to work at circumneutral pH with the use of NTA as chelating agent to keep the iron soluble during the reaction. In order to perform the optimization, DM and RCCD methodologies were applied. The optimum condition at neutral pH was tested to inactivate *E. coli* and total coliform in a municipal secondary effluent sample.

2. Materials and methods

The first part of this investigation dealt with the photo-Fenton optimization at acidic pH to remove MB. To perform that set of experiments, MB solution was prepared in pure water and then treated by photo-Fenton. Before experimentation, pH of the methylene blue solutions was adjusted to 3 with HCl. After that, the Fe^{2+} (FeSO_4) was added to the solution and stirred until complete dissolution. The solution was put into a photoreactor and the photo-Fenton reaction started when H_2O_2 was added at the same time when UV lights were turned on. Photo-Fenton experiments were carried out in a 1.2-L capacity catalytic bench photoreactor with a UVA radiation system composed of three high pressure (8 W) mercury (Hg) lamps (BLBF8T5, Philips, The Netherlands) emitting at the wavelength near 365 nm and photon flux around 4.05×10^{-5} Einsteins s^{-1} . The lamps were placed inside borosilicate tubes allowing uniform irradiation and homogeneity was kept by means of a magnetic stirrer. The reaction time was set in 30 min and samples were taken at 0, 5, 10, 15, 20 and 30 min for the analysis of MB concentration by measuring the absorbance at 620 nm. The absorbance was measured in a spectrophotometer model DR/3900 (Hach, USA).

To perform the 2^3 factorial experimental designs, the influence of the three systems variables on two levels was studied. The level values of those variables were determined in preliminary tests measuring methylene blue removal. The first tested methodology was the DM. In that experimental design, 13 experiments were performed based on the 2^3 factorial experimental design. The variable and levels of the DM methodology are presented in Table 1. The second methodology, the RCCD, allows designing 15 experiments,

including the central point, which was carried out in triplicate. The variable and levels of the RCCD are presented in Table 2.

After optimization in acidic pH, the experimental design was also used to optimize the system at circumneutral pH. In this set of experiments, the chelating agent nitrilotriacetic acid (NTA) was used to form the soluble complex and avoid iron precipitation. The wastewater samples used in this work came from a pilot plant from the School

Table 1
Methylene blue degradation after 30 min of photo-Fenton treatment at acidic pH (DM). Concentrations in mg L^{-1}

Essay	DM			% Degradation
	$\text{H}_2\text{O}_2 + \text{UV} + \text{Fe}^{2+}$			
	$[\text{H}_2\text{O}_2]$	$[\text{Fe}^{+2}]$	[MB]	
1	70	2.0	20	96.3
2	100	2.0	20	95.6
3	85	2.9	20	95.0
4	85	2.3	28	94.1
5	40	2.0	20	92.3
6	55	1.1	20	92.8
7	55	1.7	11.8	96.5
8	85	1.1	20	94.0
9	85	1.7	11.8	97.4
10	55	2.9	20	95.5
11	70	2.6	11.8	97.4
12	55	2.3	28.2	58.0
13	70	1.4	28.2	72.4

Table 2
Methylene Blue degradation after 30 min of photo-Fenton treatment at acidic pH (RCCD). Concentrations in mg L^{-1}

Essay	RCCD			% Degradation
	$\text{H}_2\text{O}_2 + \text{UV} + \text{Fe}^{2+}$			
	$[\text{H}_2\text{O}_2]$	$[\text{Fe}^{+2}]$	[MB]	
1	40	1	10	96.7
2	100	1	10	95.5
3	40	3	10	97.7
4	100	3	10	98.8
5	40	1	30	90.5
6	100	1	30	92.3
7	40	3	30	92.5
8	100	3	30	95.7
9	70	2	20	96.3
10	19.57	2	20	93.8
11	120.46	2	20	96.6
12	70	0.318	20	59.6
13	70	3.682	20	95.7
14	70	2	3.18	93.8
15	70	2	36.82	86.9

of Technology of the University of Campinas (Brazil), which was composed by a hybrid reactor: septic tank - anaerobic filter. The amount of hydrogen peroxide, Fe^{2+} and the ratio $\text{NTA}:\text{Fe}^{2+}$ were the variables of the new experimental design (using only RCCD methodology).

In the preparation of the Fe^{2+} -NTA chelating solution, 500 mL of sewage was used. The pH was adjusted first to 3 using sulfuric acid (H_2SO_4) and the correct amount of Fe^{2+} was added. Then, NTA was added and the sample was homogenized for 15 min. After, the pH was slowly adjusted to 8 using sodium hydroxide (NaOH), stirring for 120 min was carried out in order to completely chelate the iron. Subsequently the volume was completed with secondary effluent sample to 1,000 mL, adjusted to pH 7 and stirred for 15 min. This strategy allows achieving almost 100% of iron chelation by NTA [23].

The disinfection experiments using photo-Fenton with NTA-Fe at neutral pH were carried out with the best condition obtained in the previous optimization. For this purpose, the secondary effluent samples were inserted in the photo-reactor and treated by photo-Fenton using the complex Fe^{2+} -NTA. Thus 10 mL samples were taken at 0, 30, 45, 60 min to verify the efficiency of photo-Fenton with Fe^{2+} -NTA for disinfection. The disinfection rate was evaluated by the analysis of *Escherichia coli* and total coliforms inactivation by means of Collilert® test.

3. Results and discussion

3.1. Optimization at acidic pH

The first part of the optimization had the objective to test different operational conditions in order to find the optimum condition to remove MB from aqueous solutions by photo-Fenton at acidic pH. Color/MB removal in this case was used indirectly to measure the HO^\bullet formation during the

treatment since MB is highly reactive with HO^\bullet . The determination of the optimized condition at acidic pH is important to compare with the optimized at neutral pH since chelated iron usually loose its catalyst efficiency in comparison with the soluble form.

The response of the factorial designs of photo-Fenton treatment at pH = 3 was MB removal percentage after 30 min. To ensure that our results were consistent, two experimental design methodologies were used (DM and RCCD). The variables and the levels were chosen according to previous experiments. Table 1 presents the results of DM optimization, which demonstrates that, as expected, the photo-Fenton at pH 3 was very efficient on MB removal. In average, MB removal reached 90.5%. H_2O_2 concentration was an important variable since higher MB removal was obtained when H_2O_2 relative concentration toward MB was higher, that is, in the experiment number 9 (Table 1). To confirm the significance of the variables, the Pareto Chart was built (Fig. 1a). In the Pareto chart, the lengths of the bars are proportional to the estimated effects value, which help compare the relative importance of the effects on the system. Fig. 1a shows that MB concentration had a significant effect on the degradation process, the negative value of (-5.67) of the most significant effect indicates that experiments with minimum concentration level of [MB] is the most efficient. At lower MB concentration, the relative H_2O_2 concentration to remove it is higher. The relative H_2O_2 concentration regarding the MB and iron concentration was proven to be significant as it can be observed in the Pareto Chart, which shows that the interaction between ($[\text{H}_2\text{O}_2]$, $[\text{Fe}^{2+}]$) and between ($[\text{MB}]$ and $[\text{H}_2\text{O}_2]$) are statistically significant.

In order to understand the influence of the H_2O_2 concentration in the process, mainly its relation with MB concentration a surface response was built (Fig. 1b). The visualization of the graphic helps in the process of optimization because it relates two variables with the response. In Fig. 1b, the

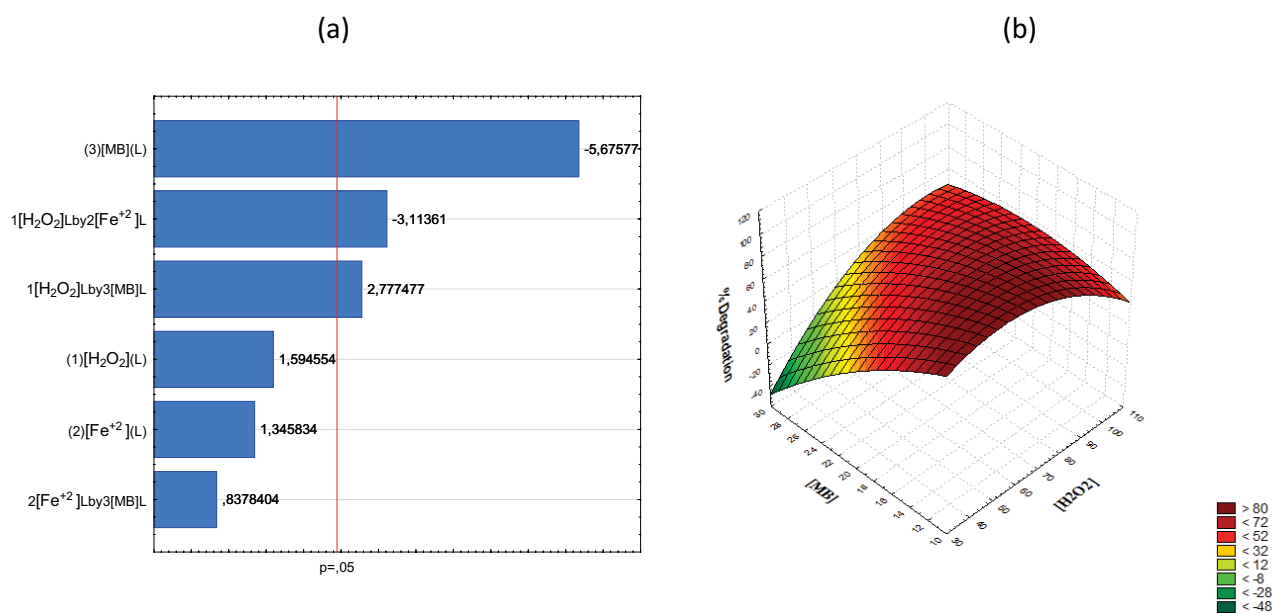


Fig. 1. (a) Pareto chart of standardized effects on MB removal; (b) response surface for MB removal as a function of MB and H_2O_2 concentration (DM).

influence of H_2O_2 concentration on different concentrations of MB is clear. At lower MB concentration, H_2O_2 seems to be in excess and the removal did not change much with H_2O_2 concentration increase. The inhibition of H_2O_2 promoted by $\text{HO}\cdot$ scavenging is evident at higher H_2O_2 concentration. When MB concentration is increased, the H_2O_2 influence is more evident since higher H_2O_2 promoted the increase of MB removal. According to the graphic, maximum MB removal is achieved near a H_2O_2 concentration near 70 and MB around 10 mg L^{-1} .

To complement the optimization study, the RCCD model was also applied. Table 2 shows the results of the optimization obtained by the RCCD model, from which it can be observed that the efficiency in MB degradation was also high (around 92%). Comparing experiments number 4 and number 12 which are the most efficient and last efficient, respectively, it is possible to verify the high influence of the $\text{H}_2\text{O}_2/\text{MB}$ concentration ratio as well as the influence of Fe^{2+} concentration. RCCD results agreed with DM in respect to the H_2O_2 relative concentration and add iron concentration also as an important variable. To properly observe the significance of each variable the Pareto chart was built (Fig. 2a). In this case, Fe^{2+} concentration was the most significant effect; the value of 8.45 of effect indicates that the maximum concentration level of Fe^{2+} is the more efficient for the use as a catalyst of the system. The surface response was also plotted using the RCCD results. Fig. 2b presets the response surface, which shows MB removal efficiency vs. the relationship between $[\text{Fe}^{2+}]$ and $[\text{MB}]$. A considerable curvature points out the optimum iron concentration around 3 mg L^{-1} , which was the optimum for that set of experiments.

3.2. Optimization at neutral pH

Once the system was optimized in acidic pH, the investigation was devoted to the optimization of variables at

neutral pH. The key factor to perform photo-Fenton at neutral pH is the solubilization of iron. One of the most usual strategies to keep iron soluble is the iron chelation [27]. In this study, NTA was used as chelant as it had in previous works showed to be able to chelate iron with good results on the removal of organic pollutants [23]. For this part of the investigation only the RCCD methodology was used. The studied variables were H_2O_2 , Fe^{2+} and NTA concentration. H_2O_2 and Fe^{2+} concentration levels were based on the results obtained on the optimization at acidic pH. In the case of NTA, the NTA/ Fe^{2+} ratio (1.5:1 M) found on literature was the base for the levels chosen in this set of experiments. MB concentration was kept at 25 mg L^{-1} and 17 experiments were performed and analyzed inside the RCCD methodology, which in that case had central point. The central point was measured in triplicate in order to obtain the experimental error (± 0.09) (Table 3).

It was remarkable that the tested variables were not significant on the used levels, as observed in the Pareto chart (Fig. 3a). At neutral pH, the complex NTA-Fe had a very low catalytic capacity in comparison with the system with free iron. When iron was on its chelated form, the influence of other variables such as the H_2O_2 concentration was reduced. In this case, it shows the existence of an important, but not statistically significant, effect between Fe^{2+} concentration and NTA. It is very close to the level of significance ($p = 0.5$) and deserves attention.

In order to assess the relation between iron and H_2O_2 concentrations in the process using NTA-Fe, a response surface graph was constructed (Fig. 3b). The H_2O_2 effect on the production of $\text{HO}\cdot$ radicals is influenced by the chelated iron concentration. At low iron concentration, the H_2O_2 is directly proportional to the augment of MB degradation. However, when the chelated iron concentration is increased, the increase of H_2O_2 did not improve the efficiency of the process. The inhibition of $\text{HO}\cdot$ formation in

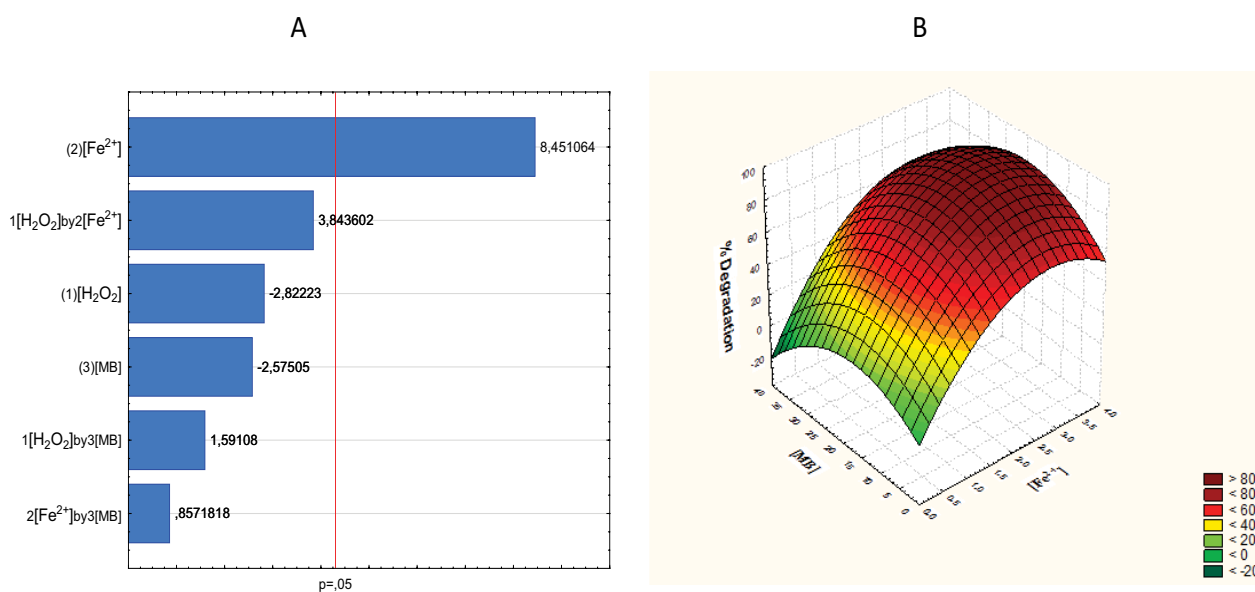


Fig. 2. (a) Pareto chart of standardized effects on MB removal (RCCD); (b) response surface for MB removal as a function of MB and Fe^{2+} concentration (RCCD).

Table 3
Percentage of Methylene Blue degradation by photo-Fenton at neutral pH

Essay	(RCCD). Concentration in mg L ⁻¹			% Degradation
	H ₂ O ₂ + UV + Fe ²⁺			
	[H ₂ O ₂]	[Fe ²⁺]	[NTA]/[Fe ²⁺]	
1	40	1	1.5	0.2
2	100	1	1.5	7.7
3	40	2	1.5	6.7
4	100	2	1.5	8.5
5	40	1	2	8.2
6	100	1	2	8.8
7	40	2	2	7.4
8	100	2	2	5.8
9	70	2	1.75	6.0
10	70	2	1.75	5.8
11	70	2	1.75	5.9
12	19.5	2	1.75	2.3
13	120.5	2	1.75	2.2
14	70	0.318	1.75	7.3
15	70	3.682	1.75	0.2
16	70	2	1.33	7.7
17	70	2	2.17	6.7

high iron concentration could be related to the presence of high concentration of the chelant agent (NTA), which may consume the produced radicals and disturb the system. The NTA concentration seems to act as scavenging at higher concentration.

Fig. 4 shows the degradation curve of MB under the best conditions achieved at acidic and neutral pH. It is clear that after 30 min of treatment the MB degradation at acidic

pH is more efficient than at neutral pH. A possible explanation for the very low removal of MB at neutral pH is the HO[•] scavenging potential of NTA along with the reduction of efficiency of chelated iron when compared with it in the soluble form at acidic pH.

3.3. Application of photo-Fenton using NTA–Fe for wastewater disinfection

Using the best results of the photo-Fenton optimization at neutral pH, a set of runs were carried out to verify its efficiency in disinfection even if the MB removal was limited. The experiments were carried out at laboratory scale with a secondary effluent coming from a pilot wastewater treatment plant of the school of Technology of the University of Campinas (Brazil). The pilot plant was composed of a hybrid reactor (septic tank and anaerobic filter). The experiments were performed for 60 min, in which samples of 10 mL were withdrawn at different reaction times (0, 30, 45 and 60 min). Afterwards, *E. coli* and total coliforms were measured by the Collilert® method.

Fig. 5 presents the inactivation of total coliforms and *E. coli* using the best conditions provided by the results

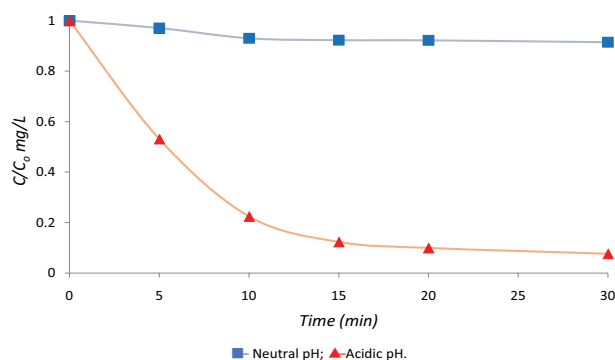


Fig. 4. Degradation curves of MB at acidic and neutral pH.

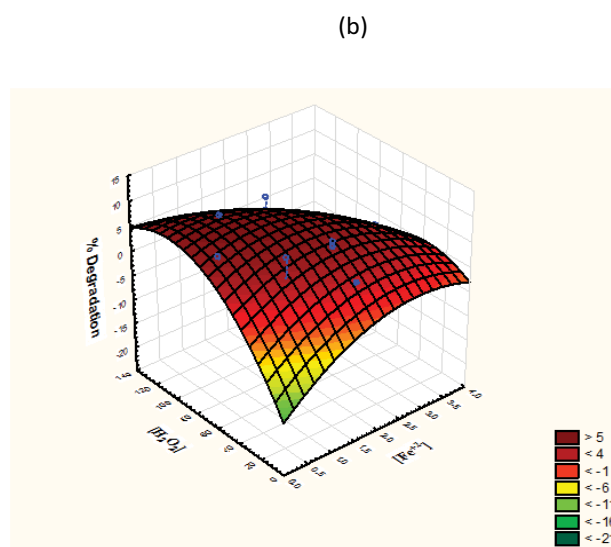
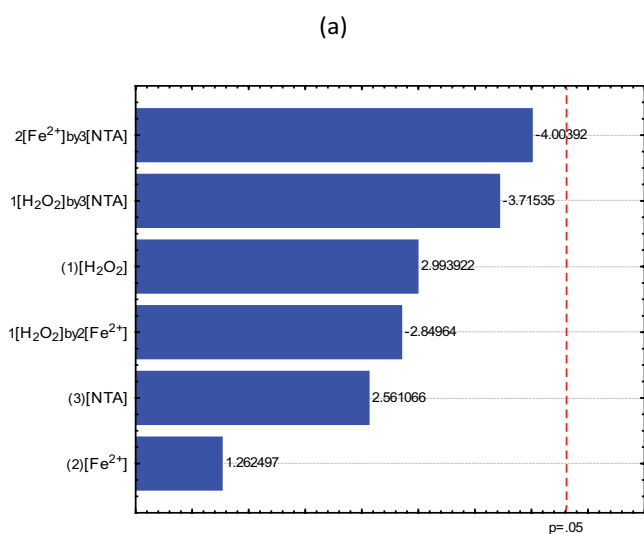


Fig. 3. (a) Pareto chart of standardized effects on MB removal (RCCD) at neutral pH. (b) Response surface for MB removal (RCCD) at neutral pH.

of the optimization. Although the best condition for the optimization of photo-Fenton at neutral pH was not able to remove MB from water, when the same condition was tested to inactivate the bacteriological indicators it was able to inactivate the microorganisms. Both *E. coli* and total coliforms were constantly inactivated during the reaction time. Total coliform was the more resistant bacteria; however, at the end of the treatment time the inactivation percentage was higher than 60%. In the case of *E. coli*, almost 100% was achieved after 60 min of photo-Fenton treatment using Fe/NTA at neutral pH. A possible explanation for the reduction of more than 4 logs for total coliforms and 6 logs for *E. coli* at the end of 60 min of treatment while no MB being affected for the same experimental condition may be due different radicals formed during the photo-Fenton using NTA-Fe when compared to it carried out at acidic pH. NTA-Fe complex may form radicals with low reactivity with MB but enough to promote the inactivation of the cited bacteria. Table 4 shows the percentage of MB removal and bacteria inactivation in different photo-Fenton conditions. The optimization of the system importantly increased color removal in both acidic and neutral pH, however the percentage of

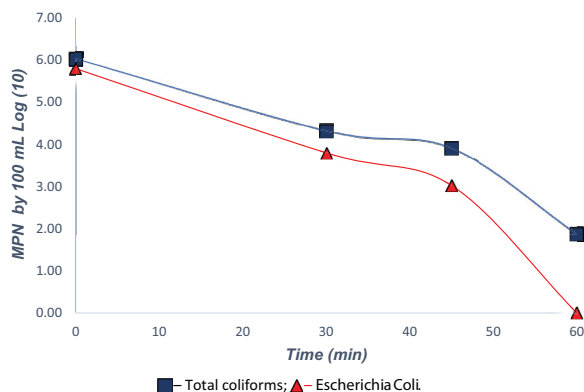


Fig. 5. Disinfection curve during treatment with photo-Fenton using Fe/NTA at neutral pH.

Table 4
Removal of MB in photo-Fenton at acidic pH and disinfection at neutral pH using NTA-Fe

Processes	Methylene blue removal		
	Best result	Worst result	
Acidic pH	% Removal	95.6	58.0
	Final concentration (mg L ⁻¹)	0.04	0.42
Neutral pH [NTA-Fe]	% Removal	8.5	0.2
	Final concentration (mg L ⁻¹)	0.92	0.99
Processes	Disinfection		
		<i>E. coli</i>	Total coliforms
Neutral pH [NTA-Fe]	% Removal	99.9	68.8
	MPN log(10)	0.00	1.88

MB removal was very low at neutral pH using the complex NTA-Fe instead of soluble Fe²⁺. Concerning the disinfection, the photo-Fenton using the NTA-Fe complex was able to inactivate around 100% of the bacteriological indications at the end of the reaction time.

4. Conclusion

The RCCD and DM methodologies allowed the optimization of photo-Fenton variables with a reduced number of experiments. The optimization at acidic pH was effective to improve MB removal from water. When the optimization was tested in the system at circumneutral pH with the use of the NTA-Fe complex instead of Fe, the best results had a very limited MB removal efficiency. However, when the optimized condition of the photo-Fenton with NTA-Fe was used to disinfect a wastewater sample, a high level of inactivation was achieved. It seems that the produced radicals with the NTA-Fe complex form radicals able to inactivate bacteria while their efficient in color removal is very limited. A possible drawback of the system is related with the quantity of NTA used in the system, since high concentrations of it may consume the formed radicals and consequently disturb the treatment. The application of photo-Fenton using NTA-Fe to disinfect municipal wastewater was promising since that strategy allowed to perform the treatment at circumneutral pH. However, a careful evaluation of NTA quantity and preparation of the complex should be taken into account for a correct and efficient disinfection.

Acknowledgements

This work was supported by the Sao Paulo Research Foundation (FAPESP) grant [2014/17774-1], the Brazilian National Council for Scientific and Technological Development (CNPq) grants [424395/2016-9] and [308914/2017-1].

References

- [1] C. Caretti, C. Lubello, Wastewater disinfection with PAA and UV combined treatment: a pilot plant study, *Water Res.*, 37 (2003) 2365–2371.
- [2] J. Koivunen, H. Heinonen-Tanski, Inactivation of enteric microorganisms with chemical disinfectants, UV irradiation and combined chemical/UV treatments, *Water Res.*, 39 (2005) 1519–1526.
- [3] B.S. Souza, R.F. Dantas, A. Cruz, C. Sans, S. Esplugas, M. Dezotti, Photochemical oxidation of municipal secondary effluents at low H₂O₂ dosage: study of hydroxyl radical scavenging and process performance, *Chem. Eng. J.*, 237 (2014) 268–276.
- [4] J.A. Malvestiti, R.F. Dantas, Influence of industrial contamination in municipal secondary effluent disinfection by UV/H₂O₂, *Environ. Sci. Pollut. Res.*, 13 (2019) 13286–13298.
- [5] J.B. Safarzadeh-Amiri, J.R. Bolton, S.R. Cater, The use of iron in advanced oxidation processes, *J. Adv. Oxid. Technol.*, 1 (1996) 18–26.
- [6] W.P. Ting, M.C. Lu, Y.H. Huang, The reactor design and comparison of Fenton, electro-Fenton and photoelectron-Fenton processes for mineralization of benzene sulfonic acid (BSA), *J. Hazard. Mater.*, 156 (2008) 421–428.
- [7] A. Babuponnusami, K. Muthukumar, Advanced oxidation of phenol: a comparison between Fenton, electro-Fenton, sono-electro-Fenton and photo-electro-Fenton processes, *Chem. Eng. J.*, 183 (2012) 1–9.
- [8] S. Malato, J. Blanco, M.I. Maldonado, I. Oller, W. Gernjak, L. Pérez-Estrada, Coupling solar photo-Fenton and biotreatment

- at industrial scale: main results of a demonstration plant, *J. Hazard. Mater.*, 146 (2007) 440–446.
- [9] S. Malato, P. Fernández-Ibáñez, M.I. Maldonado, J. Blanco, W. Gernjak, Decontamination and disinfection of water by solar photocatalysis: recent overview and trends, *Catal. Today*, 147 (2009) 1–59.
- [10] A. Zapata, I. Oller, L. Rizzo, S. Hilgert, M.I. Maldonado, J.A. Sánchez-Pérez, S. Malato, Evaluation of operating parameters involved in solar photo-Fenton treatment of wastewater: interdependence of initial pollutant concentration, temperature and iron concentration, *Appl. Catal., B*, 97 (2010) 292–298.
- [11] L. Santos-Juanes, J.L.G. Sánchez, J.L.C. López, I. Oller, S. Malato, J.A.S. Pérez, Dissolved oxygen concentration: a key parameter in monitoring the photo-Fenton process, *Appl. Catal., B*, 104 (2011) 316–323.
- [12] A.C. Reina, S. Miralles-Cuevas, J.L.C. López, J.A.S. Sánchez, Pyrimethanil degradation by photo-Fenton process: influence of iron and irradiance level on treatment cost, *Sci. Total Environ.*, 605 (2017) 230–237.
- [13] W.G. Barb, J.H. Baxendale, P. George, K.R. Hargrave, Reactions of ferrous and ferric ions with hydrogen peroxide. Part 3 - Reactions in the presence of α : α' -dipyridyl, *Trans. Faraday Soc.*, 51 (1955) 935–946.
- [14] C. Walling, Fenton's reagent revisited, *Acc. Chem. Res.*, 8 (1975) 125–131.
- [15] J.J. Pignatello, Dark and photoassisted iron (3+)-catalyzed degradation of chlorophenoxy herbicides by hydrogen peroxide, *Environ. Sci. Technol.*, 26 (1992) 944–951.
- [16] P. Villegas-Guzman, S. Giannakis, S. Rtimi, D. Grandjean, M. Bensimon, L.F. Alencastro, R. Torres-Palma, C. Pulgarin, A green solar photo-Fenton process for the elimination of bacteria and micropollutants in municipal wastewater treatment using mineral iron and natural organic acids, *Appl. Catal., B*, 219 (2017) 538–549.
- [17] M.M. Rashad, A.A. Ibrahim, D.A. Rayan, M.M.S. Sanad, I.M. Helmy, Photo-Fenton-like degradation of Rhodamine B dye from waste water using iron molybdate catalyst under visible light irradiation, *Environ. Nanotechnol. Monit. Manage.*, 8 (2017) 175–186.
- [18] Y. Sun, J.J. Pignatello, Chemical treatment of pesticide wastes. Evaluation of iron (III) chelates for catalytic hydrogen peroxide oxidation of 2, 4-D at circumneutral pH, *J. Agric. Food Chem.*, 40 (1992) 322–327.
- [19] P. Valero, S. Giannakis, R. Mosteo, M.P. Ormad, C. Pulgarin, Comparative effect of growth media on the monitoring of *E. coli* inactivation and regrowth after solar and photo-Fenton treatment, *Chem. Eng. J.*, 313 (2017) 109–120.
- [20] X. Feng, Y. Chen, Y. Fang, X. Wang, Z. Wang, T. Tao, Y. Zuo, Photodegradation of parabens by Fe (III)-citrate complexes at circumneutral pH: matrix effect and reaction mechanism, *Sci. Total Environ.*, 472 (2014) 130–136.
- [21] A. De Luca, R.F. Dantas, S. Esplugas, Assessment of iron chelates efficiency for photo-Fenton at neutral pH, *Water Res.*, 61 (2014) 232–242.
- [22] P. Villegas-Guzman, J. Silva-Agredo, O. Florez, A.L. Giraldo-Aguirre, C. Pulgarin, R.A. Torres-Palma, Selecting the best AOP for isoxazolyl penicillins degradation as a function of water characteristics: effects of pH, chemical nature of additives and pollutant concentration, *J. Environ. Manage.*, 190 (2017) 72–79.
- [23] A. De Luca, R.F. Dantas, S. Esplugas, Study of Fe (III)-NTA chelates stability for applicability in photo-Fenton at neutral pH, *Appl. Catal., B*, 179 (2015) 372–379.
- [24] S.L.C. Ferreira, A.S. Queiroz, M.S. Fernandes, H.C. Santos, Application of factorial designs and Doehlert matrix in optimization of experimental variables associated with the pre-concentration and determination of vanadium and copper in seawater by inductively coupled plasma optical emission spectrometry, *Spectrochim. Acta Part B*, 57 (2002) 1939–1950.
- [25] S.L.C. Ferreira, R.E. Bruns, E.G.P. Silva, W.N.L. Santos, C.M. Quintella, J.M. David, J.B. Andrade, M.C. Breitzkreitz, I.C.S.F. Jardim, B.B. Neto, Statistical designs and response surface techniques for the optimization of chromatographic systems, *J. Chromatogr. A*, 1158 (2007) 2–14.
- [26] J. Malvestiti, E. Fagnani, D.C. Simao, R.F. Dantas, Optimization of UV/H₂O₂ and ozone wastewater treatment by experimental design methodology, *Environ. Technol.*, 40 (2018) 1910–1922.
- [27] P. Villegas-Guzman, S. Giannakis, R.A. Torres-Palma, C. Pulgarin, Remarkable enhancement of bacterial inactivation in wastewater through promotion of solar photo-Fenton at near-neutral pH by natural organic acids, *Appl. Catal., B*, 205 (2017) 219–227.